NJC

RSC Publishing

PAPER

View Article Online
View Journal | View Issue

Cite this: *New J. Chem.*, 2013, **37**, 2541

Solvent free synthesis, characterization, anticancer, antibacterial, antifungal, antioxidant and SAR studies of novel (*E*)-3-aryl-1-(3-alkyl-2-pyrazinyl)-2-propenone†

Bheru Singh Kitawat,[a] Man Singh*[a] and Raosaheb Kathalupant Kale[ab]

Received (in Montpellier, France) 24th March 2013, Accepted 28th May 2013

DOI: 10.1039/c3nj00308f

www.rsc.org/njc

Two series of novel (*E*)-3-aryl-1-(3-alkyl-2-pyrazinyl)-2-propenones (**3a–3f** and **3g–3l**) have been synthesized by the Claisen–Schmidt condensation reaction between 2-acetyl-3-alkyl pyrazine (0.005 mol, **1a–1b**) and *para*-substituted aromatic aldehydes (0.005 mol, **2a–2f**) under solvent-free K_2CO_3 solid supported microwave environment, with 90–95% yield. The structures were confirmed by FTIR, ^{1}H NMR, ^{13}C NMR, LCMS (Q-TOF) and elemental analysis. The mean surface roughness values (R_a) of 10.59 and 10.87 nm for **3c** and **3i**, respectively, were measured with AFM. Compounds were tested for their *in vitro* anticancer activity against the MCF-7 cell line using sulforhodamine B (SRB) assay protocols to estimate cell growth and compared with adriamycin. Compound **3i** containing *p*-Br on the phenyl ring expressed promising anticancer activity ($GI_{50} \leq 0.1$ μM). The cytotoxicity (LC_{50}) was found in the range of 86 to >100 μM as compared to that of the standard (LC_{50} = 89 μM). Also, compounds were screened for *in vitro* antibacterial and antifungal activities, and the most prominent effects were observed with **3a**, **3c**, **3d** and **3e** against gram-positive and gram-negative strains. Compounds **3a–3l** showed 30–66% antioxidant activities, determined by 2,2-diphenyl-1-picrylhydrazyl (DPPH) free radical method. The viscosity as a transport property was studied for their entire composition range at 298.15 K. Data were regressed against concentration for limiting viscosity and noted as **3h** > **3g** > **3i** = **3l** > **3k** > **3a** > **3j** > **3f** > **3e** > **3c** > **3d** > **3b**.

Introduction

Pyrazine derivatives comprise an important class of aromatic fragrances[1,2] and are relevant components of the aromas of many fruits, vegetables, wines and natural products.[1,3] Pyrazine derivatives are known for their uses as versatile synthetic intermediates, and for their cyclooxygenase enzyme (COX-2) inhibiting, relaxing cardiovascular, antithrombotic, anti-aggregation, and analgesic effects.[4,5] Some reported imidazo[1,2-*a*]pyrazine derivatives are found to decrease the expression of glycoprotein (GP)Ib in Dami cells while others enhanced that of GPIIb/IIIa and also inhibited the proliferation of the human erythroleukemia (HEL) cell line.[6] Tetramethylpyrazine is used for the treatment of ischemic stroke permeate, blood–brain barrier and also enrich the brainstem and decrease nitric oxide production in human polymorphonuclear leukocytes.[7] The aminopyrazine derivatives were found to inhibit the activity of Syk kinase and showed inhibition of LAD2 cell degranulation while some have binding affinity to hepatic cytochrome P450 2E1.[8,9] Because of the wider applications of pyrazine and its derivatives, their synthesis has been a centre of attraction for researchers over the years, especially in medicinal chemistry for designing structural analogues of bioactive heterocyclic compounds with a better pharmacological profile. In the search for novel agents with better pharmacokinetic properties, potency and lower side effects, a large number of chalcone derivatives have been synthesized and several of them have shown promising biological activities. Chalcones are prominent secondary metabolites and precursors of flavonoids.[10] The presence of enone functionality (–C(O)CH═CH–) in the chalcone moiety has shown an array of biological activities such as antimicrobial,[11] anti-inflammatory,[11,12] antiplatelet,[13] antimalarial,[14] anticancer,[15,16] antileishmanial,[17] antioxidant,[11] antifungal,[18] inhibition of leukotriene B4,[19] anti-HIV[20] anti-tuberculosis[21] and also agrochemical[22] activities have been reported. Chalcones are significant precursors in the synthesis of numerous biologically

[a] *School of Chemical Sciences, Central University of Gujarat, Gandhinagar-382030, India. E-mail: mansingh50@hotmail.com; Fax: +91-079-232-60076; Tel: +91-079-232-60210*

[b] *School of Life Sciences, Jawaharlal Nehru University, New Delhi-110067, India*

† Electronic supplementary information (ESI) available: Copies of ^{1}H and ^{13}C NMR spectra are given in ESI. See DOI: 10.1039/c3nj00308f

important pyrimidines, isoxazolines, pyrazolines, flavonoids and other heterocycles.[23–25]

Conventionally, chalcones are synthesized by the Claisen–Schmidt condensation reaction of substituted aldehydes and ketones using strong acid or base or high cost catalysts like $LiNO_3$/natural phosphate, Amberlyst-15, bamboo char sulfonic acid, $SOCl_2$/EtOH, $Cu_3(BTC)_2(H_2O)_3$, zinc oxide, and Zn–Al hydrotalcite adhere ionic liquid in organic solvents, which not only required longer time, high temperature, inert environment but also involve typical workup procedures with lesser yield.[26–32]

On the other hand, for benign synthesis, modern research and trends require advanced techniques for synthesis of various biologically potent compounds with limited resources.[33–35] Thereby, microwave assisted organic synthesis (MAOS) has gained the consideration of chemists due to its inimitable advantages, such as shorter reaction times, cleaner products, higher yields, simplicity in operation and being a potential alternative to accomplish efficient synthesis.[33–35] Further, solvent-free reactions are of great importance in organic synthesis as it bring down the experimental costs due to simplification of the work-up and reduction of environmental pollution.[33,34] The MAOS is termed as e-synthesis, because it is easy, effective, economical, efficient and environment friendly.[23–25]

Thus, keeping in view the high degree of biomedical activities expressed by pyrazine and chalcone derivatives, in the present work, the focus has been drawn on designing new structural entities of chalcones by incorporating pyrazine and aromatic *para*-substituted aldehydes into chalcone scaffolds to evaluate the potential effects on biological activity, particularly for anticancer, antimicrobial and antioxidant activities. Synthesis of the title compounds for developing an easily reproducible methodology under solvent free K_2CO_3 solid supported microwave environment has been adopted. The easy work-up of the products, rapid reaction, and mild conditions are notable features of this method. Further, to extend the scope of the reaction, the synthesis of other alkyl substitute pyrazines for chalcone synthesis and their chemical reactions for pyrazoline, pyrimidine and isoxazoline synthesis along with anticancer and antimicrobial activities are under consideration in our laboratory.

To the best of our knowledge, no one has yet considered pyrazines as potential molecules for chalcone synthesis with their anticancer, antibacterial, antifungal and antioxidant activities.

Results and discussion

Chemistry

Two novel series of (*E*)-3-aryl-1-(3-alkyl-2-pyrazinyl)-2-propenone (**3a–3l**) have been synthesized by Claisen–Schmidt condensation reaction between an equimolar ratio (0.005 mol) of 2-acetyl-3-alkyl pyrazine (**1a–1b**) and *para*-substituted aldehydes (**2a–2f**) by conventional and MAOS methodologies, as shown in Scheme 1. Comparative data of both methods are given in Table 1. The authenticity of the products **3a–3l** was confirmed by FTIR, ^{1}H NMR, ^{13}C NMR and LCMS (Q-TOF) spectral data (see ESI†).

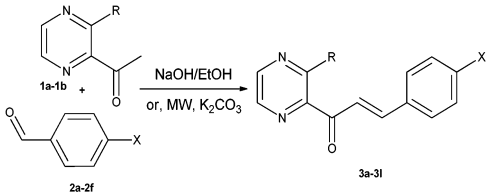

R = -CH3, -CH2CH3, X = -F,-Cl,-Br, -NO2, -N(CH3)2,-OCH2C6H5

Scheme 1 Synthesis of (*E*)-3-aryl-1-(3-alkyl-2-pyrazinyl)-2-propenones (**3a–3l**).

Table 1 Various substituents used in the synthesis and comparison between conventional and MW methods

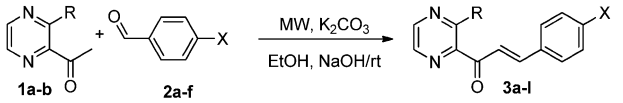

Entry	R	X	Method A time (h)/yield (%)	Method B time (min)/yield (%)	m.p. (°C)	Onset point[a] (°C)
3a	$-CH_3$	–F	6.0/84	6.0/91	113–115	113.71
3b	$-CH_3$	–Cl	5.5/87	8.0/95	128–130	128.67
3c	$-CH_3$	–Br	5.5/85	9.5/91	135–137	136.92
3d	$-CH_3$	$-NO_2$	6.0/88	6.5/90	191–193	192.22
3e	$-CH_3$	$-N(CH_3)_2$	7.0/86	8.5/93	113–115	113.34
3f	$-CH_3$	$-OCH_2Ph$	7.0/88	10/91	140–142	139.41
3g	$-C_2H_5$	–F	5.5/87	7.5/92	105–107	105.27
3h	$-C_2H_5$	–Cl	5.0/86	9.5/91	114–116	115.05
3i	$-C_2H_5$	–Br	6.5/83	6.5/94	95–97	95.70
3j	$-C_2H_5$	$-NO_2$	6.5/86	8.5/92	199–201	199.59
3k	$-C_2H_5$	$-N(CH_3)_2$	5.0/83	6.5/92	105–107	105.88
3l	$-C_2H_5$	$-OCH_2Ph$	5.0/88	8.0/94	118–120	118.20

[a] Onset point measured with differential scanning calorimeter and compared with m.p., which are in similar range.

The FTIR absorption peaks of compounds **3a–3l** at 3103–3000 cm^{-1} are attributed to –CH stretching of aromatic ring. The peaks at 2920, 2982 and 2822–2932 cm^{-1} are due to –CH stretching of methyl and ethyl chains of the pyrazine ring and $-N(CH_3)_2$ of **3e** and **3k**. The sharp shoulder at 1655 to 1692 cm^{-1} confirmed the –C═O stretching vibration of the chalcone backbone chain in **3a–3l**. The peaks in the 1590 to 1664 cm^{-1} region are the –C═N stretching vibrations of the pyrazine ring. The peaks at 1557, 1593, 1508 and 1533 cm^{-1} are due to –C═C– stretching and bending vibrations of the aromatic ring, respectively. Peaks at 1516 and 1344 cm^{-1} due to Ar–NO_2, 1373 and 1332 cm^{-1} due to Ar–$N(CH_3)_2$, and 1247 and 1177 cm^{-1} due to the stretching vibration of the Ar–C–O–C– ester bond linkage are observed. The peaks at 981 and 1014 cm^{-1} in **3a–3l**, due to stretching of –C(O)CH═CH– linkage, confirm the formation of an α,β-unsaturated ketonic bond.

In the ^{1}H NMR spectra of **3a–3l**, H_α and H_β appeared as doublets due to olefinic vicinal coupling at δ = 7.33–7.89 ppm and δ = 8.22–7.39 ppm, respectively, with coupling constant values J = 13–17 Hz between them, which agrees with *E*-propenones.[16] The ^{13}C NMR spectra provided a final structural elucidation of **3a–3l**. Thus, the signals for C_α and C_β were in the range of δ = 118.02–124.20 ppm, the signal for C_β appears at δ = 140.66–145.38 ppm, while –C═O carbon appears at δ = 190.04–191.12 ppm (see ESI†).

The UV-vis absorption properties of **3a–3l** at r.t. were recorded at a molar concentration 3×10^{-3} in ethanol. The absorption spectra of each compound exhibits intense absorption bands which are due to the $\pi \rightarrow \pi^*$ transition of the conjugated backbone.[36] The *para*-substituted effect on the absorption of electron donating and electron withdrawing groups is seen from the UV absorption values. The spectral shapes of the compounds are very similar because these compounds possess similar structures. Compounds **3a–3l** exhibit two prominent bands appearing at 305, 345 nm (**3a**), 305, 330 nm (**3b**), 315, 375 nm (**3c**), 315, 390 nm (**3d**), 310, 510 nm (**3e**) 310, 415 nm (**3f**), 310, 365 nm (**3g**), 315, 375 nm (**3h**), 305, 375 nm (**3i**), 295, 380 nm (**3j**), 295, 510 nm (**3k**) and 250, 420 nm (**3l**), respectively. The maximum absorption band is red-shifted from 310 to 510 nm and from 295 to 510 nm for **3e** and **3j**, respectively, due to the lone electron pair donating nature of nitrogen in $-N(CH_3)_2$ to the aromatic ring which makes the conjugated-system of molecules become larger and band shift towards red shift is attributed to the $n \rightarrow \pi^*$ transition. Compounds **3f** and **3l**, which have one more phenyl ring in their structures than the rest of compounds, lead to a bathochromic shift of about 95 and 90 nm (**3e** *versus* **3f** and **3k** *versus* **3l**). This result is in accordance with the weak donor character of the phenyl ring. The electron withdrawing groups (4-F, 4-Cl, 4-Br and 4-NO_2) at the *para*-position lead to a bathochromic shift as compared to **3e**, **3f**, **3k** and **3l**. The first transition is ascribed to a localized aromatic $\pi \rightarrow \pi^*$ transition and the later is an $n \rightarrow \pi^*$ transition.[37] Thus, these differences might result from the different conjugation degrees and different electron effects of the compounds.[38]

Biological evaluation

Anticancer study

The *in vitro* anticancer activity of compounds **3a–3l** was performed on human malignant cell line MCF-7 at four dose levels of 0.1, 1.0, 10 and 100 μM mL^{-1} in dimethyl sulfoxide (DMSO) and the test consisted of a 48 h continuous drug exposure protocol using sulforhodamine B (SRB) assay to estimate cell growth.[39] Appropriate positive controls were run in each experiment and each experiment was repeated thrice and a graph was plotted against percentage control growth and concentration (Fig. 1) to calculate various parameters.

Results are given in terms of GI_{50} (concentration of drug that produces 50% inhibition of the cells), TGI (concentration of the drug that produces total inhibition of the cells) and LC_{50} (concentration of the drug that kills 50% of the cells) values that were calculated from the mean graph. Adriamycin (ADR), which is a chemotherapy drug often used to kill cancer cells, was used as the standard anticancer drug.[40] Reported parameters are given in Table 2.

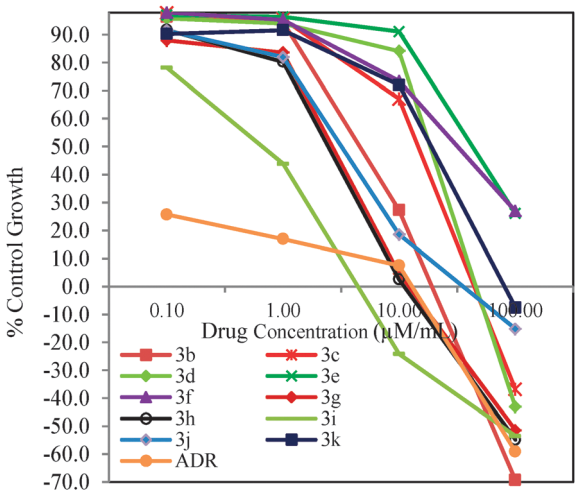

Fig. 1 Curve between percentage control growth and concentrations of drugs on MCF 7 cell line.

As shown in Table 2, compounds which have less than 0.1 μM GI_{50} are considered as anticancer active. Compound **3i**, having 4-Br on the phenyl ring, showed promising anticancer activity against the MCF7 cell line with a GI_{50} value of less than 0.1 μM. The GI_{50} values of the other compounds were found to be more than 10 μM and the trend of GI_{50} is noted as **3i** = **ADR** > **3h** > **3g** > **3b** > **3j** > **3c** > **3d** > **3k** > **3f** > **3e**. Replacing $-CH_2CH_3$ (**3i**) by $-CH_3$ (**3c**) of 4-Br substituted compounds is noted to lower the activity. The higher GI_{50} values in both series of **3e** (GI_{50} = 67.5 μM) and **3k** (GI_{50} = 40.7 μM) having $-N(CH_3)_2$ at the *para*-position on the phenyl ring may be attributed to the two methyl groups attached with nitrogen that increased the hydrophobicity leading to a decrease in the anticancer activity as compared to the halogens at the *para*-positions of the phenyl ring.

Table 2 *In vitro* testing expressed as growth inhibition of human cancer cell line MCF7 of **3a–3l**[a]

Entry	LC_{50}	TGI	GI_{50}
3a	ND*	ND	ND
3b	86	53.2	20.3
3c	>100	71.8	33.3
3d	>100	70.1	34.3
3e	>100	>100	67.5
3f	>100	>100	64.3
3g	95.9	54.5	13.1
3h	93.2	52.9	12.5
3i	92	40.3	<0.1
3j	>100	79.2	22.2
3k	>100	92.5	40.7
3l	ND	ND	ND
STD**	89	25.9	<0.1

[a] Data are the mean values of three replicates for each concentration (0.1, 1.0, 10, 100 μM mL^{-1}). DMSO was used as a vehicle. LC_{50} = concentration of drug causing 50% cell kill. TGI = concentration of drug causing total inhibition of cell growth. GI_{50} = concentration of drug causing 50% inhibition of cell growth. STD** = adriamycin, positive control drug for MCF7 cell line. ND* = activity not done.

Introduction of an ethyl group on the pyrazine ring lowers the GI_{50} value as compared to methyl-substituted pyrazine (Table 2). The TGI values of **3b–3l** are higher than the ADR (25.9 μM). The cytotoxicity (LC_{50}) was also investigated and found to be in good agreement from 86 to >100 μM as compared to standard drug adriamycin (LC_{50} = 89 μM). The LC_{50} values of **3b**, **3g**, **3h** and **3i** were noted as 86, 95.9, 93.2 and 92 μM, respectively, which fall in range of ADR. The LC_{50} values for other compounds were found to be more than 100 μM (Table 2). Variations in their activities have been found to be related to the electronic effects of the substituent groups at the *para* position of the phenyl rings and alkyl chains of the pyrazine rings.

Antioxidant study

In general, antioxidant compounds are capable of scavenging free radicals and for this purpose, antioxidant therapy is one of the most recent options.[41] Antioxidant activity of **3a–3l** was determined by 2,2-diphenyl-1-picrylhydrazyl (DPPH) free radical method.[41] Stock solution of DPPH free radical in ethanol (2.16 mg/50 mL) was prepared and the absorbance was recorded at 517 nm. Then, 20, 40, 60, 80, 100 μg mL^{-1} of **3a–3l** and L-ascorbic acid (AA) as standard antioxidant, were prepared in ethanol by dilution method of 100 μg mL^{-1} stock solution. 1 mL sample solution and 1 mL of stock solution of DPPH were added and put into dark conditions for up to 30 min. Then an absorbance was recorded at 517 nm and the percentage scavenging activity was calculated with the following relation and the results are plotted in Fig. 2 and given in Table 3.

$$\text{Scavenging activity (\%)} = (A_c - A_s/A_c) \times 100$$

where A_c = absorbance of DPPH, A_s = absorbance of test sample.

DPPH radical scavenging activity of the compounds was found to be good-to-moderate as compared to the standard AA. The **3a**, **3b**, **3c**, **3d**, **3g**, **3h**, **3i**, **3j** and **3l** showed an increase in % antioxidant activity within the range of 36 to 66% with an increase in concentration, while **3e**, **3f** and **3k** showed a decrease in % antioxidant activity with an increase in concentration. The lowest activity was noted for **3e** from 16.48 to 0.11% with an increase in concentration, perhaps due to the electron lone pair donating nature, while **3l** showed the highest antioxidant activity from 57.49 to 66%. Thus, the antioxidant activity of the compounds is related to their electron or hydrogen radical releasing abilities to DPPH so that they become stable diamagnetic molecules. This might be the reason for the higher or lower antioxidant activity. The L-ascorbic acid was used as a standard antioxidant with 97 to 98.50% antioxidant activity and increased with concentration (Table 3).

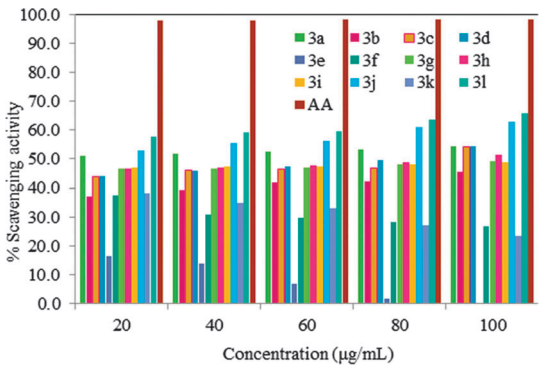

Fig. 2 Antioxidant activity of **3a–3l** determined by DPPH free radical method at various concentrations.

Table 3 Antioxidant activities of **3a–3l** determined by DPPH free radical method[a]

% Antioxidant activity					
Concentration (μg mL^{-1})					
Entry	20	40	60	80	100
3a	51.16	51.96	52.51	53.39	54.35
3b	36.93	39.32	41.93	42.27	45.45
3c	44.09	46.25	46.48	46.70	54.20
3d	44.09	45.91	47.50	49.66	54.43
3e	16.48	13.86	06.82	01.52	00.11
3f	37.39	30.68	29.77	28.30	26.93
3g	46.74	46.86	47.09	48.26	49.42
3h	46.51	47.09	47.67	49.07	51.51
3i	47.21	47.44	47.56	48.26	48.95
3j	53.10	55.41	56.26	61.12	62.94
3k	38.27	34.87	32.93	27.22	23.57
3l	57.49	59.30	59.42	63.55	65.98
AA*	97.81	98.06	98.18	98.30	98.42

[a] Data are the mean values of three replicates for each concentration. AA* = ascorbic acid as standard antioxidant compounds.

In vitro evaluation of antimicrobial activity

The *in vitro* antibacterial activities of compounds **3a–3l** were carried out using the human pathogenic gram-positive (*S. aureus*; ATCC 33591) and gram-negative (*E. coli*; ATCC 25922) bacterial strains. The antifungal activities were carried out with *C. albicans*; ATCC 14053. The ampicillin, gentamicin, and fluconazole were used as the standard drug for gram-positive, gram-negative and fungal strains, respectively. The minimum inhibitory concentration (MIC) was evaluated by the broth tube dilution method[42] using Mueller Hinton broth use as a nutrient medium to grow and to dilute the drug suspension for the test respectively. Serial dilutions of the test compounds, already dissolved in DMSO, were prepared to final concentrations of 512, 256, 128, 126, 64 and 32 μg mL^{-1}. The MIC which inhibits the visible growth after 24 h, was determined visually after incubation for 24 h, at 37 °C and pH 7.4. The lowest concentration, which showed no visible growth, was taken as an end point for MIC. The MIC level of **3a–3l** against these organisms is given in Table 4.

The data revealed that the methylpyrazine chalcones **3a**, **3c**, **3d** showed considerable antibacterial activity with MIC 64, 64 and 32 μg mL^{-1} while ethylpyrazine chalcones showed sensitive activity up to concentration 256 (**3i–3l**) and 512 (**3f–3h**) μg mL^{-1} against gram-positive strains. Further, compound **3b** and **3e** showed sensitive activity at MIC 128 μg mL^{-1}. On the basis of MIC results, it was found that compounds having methyl substitution on pyrazine and electron withdrawing groups such

Table 4 MIC values for **3a–3l** against *S. aureus*, *E. coli* and *C. albicans* strains[a]

Minimum inhibitory concentration (MIC, μg mL^{-1})			
Entry	*S. aureus*	*E. coli*	*C. albicans*
3a	64	512	>512
3b	128	>512	>512
3c	64	128	>512
3d	>32	128	>512
3e	>128	512	>512
3f	512	512	>512
3g	512	512	>512
3h	512	512	>512
3i	256	512	>512
3j	256	>512	>512
3k	256	>512	>512
3l	256	>512	>512

[a] Data are the mean values of three replicates for each concentration. The compounds were dissolved in DMSO.

as floro, chloro, bromo and nitro on the *para* position of the phenyl ring are more sensitive against gram-positive strains.

Compounds **3c** and **3d**, having 128 μg mL^{-1} MIC, are sensitive against *E. coli*, while the MIC of the rest of the compounds was found to be 512 μg mL^{-1} or greater. None of the compounds showed activity below 32 μg mL^{-1}. It was noted that an increase in alkyl chain length at the pyrazine ring lowers the antibacterial activities (Table 4). The tested compounds showed no significant effect against *C. albicans*, whereas they showed activity against *S. aureus*. The MIC values against *C. albicans* of the compounds were found to be greater than 512 μg mL^{-1}.

Atomic force microscopy study

Microstructure analysis of the compounds is generally important to understand their physicochemical role, morphology, topology and size distribution, which play significant roles in drug binding studies.[43] Topographical images of **3c** and **3i** were taken using AFM, with a uniform thin film of **3c** and **3i** in acetonitrile on a 10 × 2.5 cm glass slide. To evaporate excess solvent, the slide was kept in vacuum at r.t. for 24 h.[44] The sample was scanned using non-contact tapping mode and obtained 3D topological images (Fig. 3). The vertical and horizontal line analysis of images for **3c** and **3i** showed roughness parameters such as minimum and maximum surface value. Mean roughness (R_a) values which were found to be 10.23 and 10.89 nm, respectively, are the mean values of the surface relative to the centre plane (Table 5). The other roughness parameters like mid-value (average of maximum and minimum), mean, peak to valley of the line (Rpv, difference between minimum and maximum), root-mean-squared roughness, ten point average roughness area (Rz, is the arithmetic average of the five highest and five lowest valleys peaks in the line calculated by ten point average), skewness (Rsk) and kurtosis (Rku) values of line are given in Table 5.

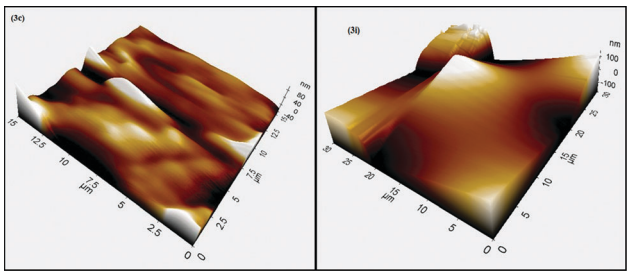

Fig. 3 Topographical surface roughness images of compound **3c** and **3i**.

Viscosity

Viscosity is a transport property which plays an important role in the fluid dynamics of drug and pharmaceutical sciences for their rheological flow and frictional force.[45] Thus, the viscosities of the compounds **3a–3l** were measured at 298.15 K from 0.002 to 0.010 molar concentrations with acetonitrile (ACN) using Borosil Mansingh Survismeter (BMS) whose procedural details are reported elsewhere[46] and calibrated using ACN. The primary viscosity data of **3a–3l** were regressed against concentration and their limiting viscosities (η^0) are plotted in Fig. 4.

The η^0 trend was noted as **3h** > **3g** > **3i** = **3l** > **3k** > **3a** > **3j** > **3f** > **3e** > **3c** > **3d** > **3b**, and from **3b** to **3f**, the η^0 decreased by approximately 1.0 time than of the ACN viscosity. The maximum viscosity of **3b** decreased from 0.345 to 0.343 mPa s. The effect of electron withdrawing and donating groups at the *para* position influenced the viscosity of ACN, depicted with experimental data. On increasing the alkyl chain length ($-CH_3$ verses $-C_2H_5$), hydrophobicity increases which in turn increases the viscosity as a result of weaker interactions. Based on this interaction, we proposed an interacting model of compound **3e** with ACN (Fig. 5).

***In silco* pharmacology and structural activity relationship (SAR) study.** To qualify compounds as a drug candidate, drug-like properties were analysed by the parameters set by Lipinski's rule of five (ClogP, solubility, molecular weight, drug likeness and drug score) using Osiris property explorer[47] and compared with some anticancer drugs listed in Table 6.

The ClogP value is used as an indicator to measure lipophilicity and also the ability to irritate the various cell membranes.[11] The ClogP values are in the range of 1.5 to 3.2, which is in close agreement with the standard drugs. The drug score values are in good agreement with the standard anticancer drug score values. Compounds **3a**, **3b**, **3c**, **3g**, **3h**, **3i** and **3l** showed good drug score values, calculated by combining all parameters. Thus, the compounds could be considered as potent lead compounds in drug discovery.

On the basis of reported biological activities, the structural activity relationship has been proposed which agreed well with the effect of substitution at the *para* position on the phenyl ring and alkyl substitution on pyrazine rings which seem responsible for lower or higher activities. Groups such as –F, –Cl, Br, $-NO_2$, $-N(CH_3)_2$ and $-OCH_2Ph$ were introduced at the *para* position on the phenyl ring along with introduction of methyl and ethyl groups at the 3-position on the pyrazine ring to introduce structural diversity. Results from the biological assay showed that, in general, electron-withdrawing groups of the phenyl ring are better for antibacterial activity, while ethyl pyrazine-based compounds are more active against anticancer

Table 5 AFM topographical mean surface parameters (nm) for **3c** and **3i**

Entry	Line	Min.	Max.	Mid	Mean	Rpv	Rq	Ra	Rz	Rsk	Rku
3c	Horizontal	−25.66	17.11	−4.28	0.00	42.77	12.45	10.59	24.75	0.40	2.01
	Vertical	−16.52	12.06	−2.23	0.00	28.59	6.80	5.23	25.05	0.88	3.40
3i	Horizontal	−31.79	17.16	−6.20	0.00	51.54	12.96	10.87	40.51	0.29	2.30
	Vertical	−16.16	19.75	0.50	0.00	33.32	9.90	8.55	6.51	−0.04	1.79

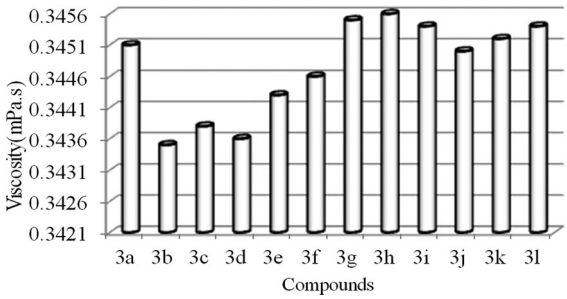

Fig. 4 Limiting viscosity of **3a–3l** in acetonitrile at 298.15 K.

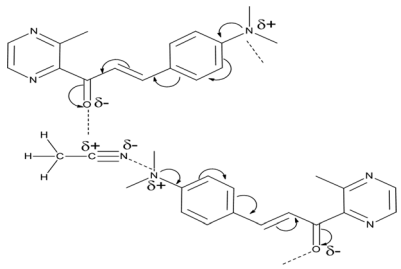

Fig. 5 Viscosity interacting model of compound **3e** with acetonitrile.

Table 6 ClogP, solubility, drug likeness and drug score values of **3a–3l** and their comparison with some standard anti-cancer drugs

Entry	ClogP	Solubility	Drug likeness	Drug score
3a	1.94	−2.96	−0.37	0.51
3b	2.49	−3.38	1.44	0.62
3c	2.58	−3.48	−1.61	0.49
3d	1.75	−3.10	−9.92	0.27
3e	1.87	−2.68	−3.54	0.17
3f	3.14	−3.98	−7.66	0.38
3g	2.29	−3.12	−0.56	0.48
3h	2.85	−3.54	1.24	0.59
3i	2.93	−3.64	−1.79	0.46
3j	2.10	−3.26	−10.09	0.26
3k	2.23	−2.84	−3.70	0.16
3l	3.50	−4.14	−7.79	0.36
Tamoxifen	5.69	−4.40	6.30	0.30
Temozolomide	−0.24	−2.57	−3.41	0.17
Lumustine	2.24	−2.54	−1.21	0.12
Carmustine	1.27	−1.67	2.76	0.20
Trimetrexate	2.15	−4.84	2.31	0.65
Silibinin	0.94	−1.82	1.97	0.90

activity. Halogens at the *para* position showed 50% antioxidant activity in comparison to other substituents. Methypyrazine-based chalcones lower the viscosity in comparison to ethylpyrazine because the hydrophobicity increases in ACN by weakening the interactions.

Conclusions

In conclusion, two novel series of pyrazine moieties containing substituted chalcones have been synthesized by a solvent-free microwave-assisted method. The solvent-free synthesis is better than the conventional method with shorter reaction time (h to min), better yield and simpler work-up. Their characterization was made using various spectral techniques. Various *in vitro* studies were performed which agreed well that **3a**, **3c**, **3d** and **3f** are sensitive against gram-positive strains, while **3a**, **3c** and **3d** also showed moderate-to-good sensitivity against gram-negative strains. Compound **3i** showed remarkable anticancer activity against the MCF7 cell line while **3b** showed effective efficacy in comparison to ADR. The compounds showed 35 to 66% antioxidant activity. The AFM study has provided a new outlook for drug loading, drug delivery, thin film formation, DNA binding or interactions of drugs and *in vivo* studies. The relationship between structural and biological properties has been explored and could be helpful in designing more potent compounds for biomedical uses in future.

Experimental

General

2-Acetyl-3-alkylpyrazine (**1a–1b**) and aldehydes (**2a–2f**) were of synthetic grade and purchased from Sigma Aldrich chemicals and used as received. The K_2CO_3, NaOH and solvents were from Rankem, India. Freshly prepared Milli pore water was used as a solvent (conductance 1×10^{-6} μS). The reactions were carried out with an Anton Paar Synthos 3000 microwave reaction system at an output power of 300 W, infrared (IR) temperature 70 °C. The reaction progress was monitored with TLC (Merck, silica GF257) using ethyl acetate/hexane (1 : 2, v/v) solvent system and spots were visualized under UV light (RICO scientific industries, Model RSUV-5). Melting points were determined on a Veego apparatus and are uncorrected. Elemental analysis was performed with Euro Vector CHNS/O analyser. FT-IR spectra were recorded in KBr pellets with a Perkin Elmer spectrum 65 FTIR spectrophotometer. Characteristic wavenumbers are given in cm^{-1}. ^1H and ^{13}C NMR spectra were recorded at r.t. in 5 mm tube using a Bruker Avance III 500 MHz spectrometer in deuterated chloroform ($CDCl_3$) and tetramethylsilane (TMS) as the internal standard. The chemical shifts are given in δ ppm and coupling constants J in Hz. Splitting patterns are described as singlet (s), doublet (d), triplet (t), quartet (q), broad (br) and multiplet (m). Mass spectral analysis was accomplished on Agilent Technologies G6520B LCMS-QTOF mass spectrometry with +ESI ionization method. The mobile phase 0.02% trifloroacetic

acid in water and acetonitrile (30 : 70 v/v) was run on an Agilent zorbax 300 SB-C18 column (3.5 μm, 4.6 × 50 mm) with flow rate of 0.5 mL min^{-1}. The absorption transition (λ_{max}) was recorded in ethanol at r.t. ranging from 200–600 nm using Analytical UV spectro 2060 plus.

Chemistry

Two different methods were used for the synthesis of (*E*)-3-aryl-1-(3-alkyl-2-pyrazinyl)-2-propenone by Scheme 1.

Method A: general procedure for the synthesis of compounds 3a–3l by conventional method

2-Acetyl-3-alkylpyrazine (**1a–1b**, 0.005 mol) and substituted aromatic aldehyde (**2a–2f**, 0.005 mol) were taken into a 50 mL round bottom flask and dissolved in 10 mL ethanol. In a clear solution, a 10% solution of NaOH was added dropwise over a time duration of 10 min, followed by stirring at r.t. Initially the reaction mass color changed from clear to light yellow with precipitate. The reaction progress was monitored by TLC with ethyl acetate/hexane (1 : 2, v/v) as eluents. After completion of the reaction followed by TLC (Table 1), the reaction mixture was poured over crushed ice, acidified with dilute HCl and the resultant precipitate was left overnight in a refrigerator. The precipitated was filtered off with a Buckner funnel on Whattman filter paper no. 42 and washed with cold water (5 × 3 mL). The wet solid was dried under vacuum and absolute dryness was checked with anhydrous copper sulphate. Compound **3a** was subjected to flash column chromatography using ethyl acetate–hexane as eluents at a ratio of 30 : 70 and 50 : 50 (v/v) on 230–400 mesh size silica gel. The overall yields of **3a–3l** were obtained as 83–88%. The products were recrystallized in ethanol/methanol/toluene to afford **3a–3l**.

Method B: general procedure for the synthesis of compounds 3a–3l using microwave-assisted method

2-Acetyl-3-alkylpyrazine (**1a–1b**, 0.005 mol), substituted aromatic aldehyde (**2a–2f**, 0.005 mol) and K_2CO_3 (2.5 g) were taken in teflon reaction vessels, mixed properly in ethyl acetate (5 mL), dried in air and irradiated at 300 W, with an IR temperature of 70 °C and a maximum pressure of 20 bar inside the vessels for completion of reactions, as given in Table 1. The progress of the reaction was followed by TLC within ethyl acetate/hexane (1 : 2, v/v) as eluents. The reaction mixture was cooled to ambient temperature and the product was extracted with ethyl acetate and concentrated under vacuum using a Buchi rotary evaporator. The overall yields of synthesized compounds were obtained as 90–95%. The compounds were recrystallized in ethanol/methanol/toluene to afford **3a–3l**.

(*E*)-3-(4-Fluorophenyl)-1-(3-methylpyrazine-2-yl)prop-2-en-1-one (3a)

Molecular formula: $C_{14}H_{11}FN_2O$; color: yellow crystals; R_f: 0.75; m.p.: 113–115 °C; λ_{max}: 305, 345; elemental analysis: calculated: C (69.41%), H (4.58%), N (11.56%), O (6.60%); found: C (69.35%), H (4.62%), N (11.50%), O (6.65%); FTIR (KBr, ν_{max} in cm^{-1}): 3047 (Ar, –CH str.), 2977, 2932 (–CH str., $–CH_3$), 1671 (–C═O), 1602 (–C═N), 1557, 1508 (–C═C–), 981(–C(O)CH═CH), 834 (1,4 substituted Ar ring); +ESIMS: calculated for $C_{14}H_{12}FN_2O^+$ 243.0855, found 243.0937; ^{1}H NMR (500 MHz, $CDCl_3$, δ ppm): 2.90 (s, 3H, $–CH_3$), 7.15–7.12 (t, 2H, J = 8.0 Hz, $H_{12,14}$), 7.72–7.69 (t, 2H, J = 7.0 Hz, $H_{11,15}$), 7.82–7.79 (d, 1H, J = 16.0 Hz, H_α), 7.95–7.92 (d, 1H, J = 16.0 Hz, H_β), 8.56 (s, 1H, H_2), 8.65 (s, 1H, H_1); ^{13}C NMR (125 MHz, $CDCl_3$, δ ppm): 23.43 (C_7, $–CH_3$), 116.19–116.02 ($C_{12,14}$, Ar ring), 122.54–122.52 (C_α, –CH═CH–), 130.73–130.66 ($C_{11,15}$, Ar ring), 131.08–131.06 (C_{10}, Ar ring), 140.69 (C_β, –CH═CH–), 143.70 (C_2, pyrazine ring), 145.67 (C_4, pyrazine ring), 147.75 (C_1, pyrazine ring), 155.16 (C_5, $C–CH_3$), 163.16 (C_{13}, C–F), 190.58 (C_8, –C═O).

(*E*)-3-(4-Chlorophenyl)-1-(3-methylpyrazin-2-yl)prop-2-en-1-one (3b)

Molecular formula: $C_{14}H_{11}ClN_2O$; color: light yellow crystals; R_f = 0.74; m.p.: 128–130 °C; λ_{max}: 305 and 330 nm; elemental analysis: calculated: C (65%), H (4.29%), N (10.83%), O (6.18%); found: C (65.10%), H (4.22%), N (10.93%), O (6.23%); FTIR (KBr, ν_{max} in cm^{-1}): 3030 (Ar, –CH str.); 2981, 2924 (–CH str., $–CH_3$); 1671 (–C═O), 1602 (–C═N), 1565, 1524 (–C═C–), 981 (–C(O)CH═CH), 818 (1,4 substituted Ar ring); +ESIMS: calculated for $C_{14}H_{12}ClN_2O^+$ 259.0559, found 259.0650; ^{1}H NMR (500 MHz, $CDCl_3$, δ ppm): 2.89 (s, 3H, $–CH_3$), 7.40–7.39 (d, 2H, J = 8.0 Hz, $H_{12,14}$), 7.62–7.61 (d, 2H, J = 8.0 Hz, $H_{11,15}$), 7.79–7.75 (d, 1H, J = 16.0 Hz, H_α), 7.987.95 (d, 1H, J = 16.0 Hz, H_β), 8.54 (s, 1H, H_2), 8.63 (s, 1H, H_1); ^{13}C NMR (125 MHz, $CDCl_3$, δ ppm): 23.44 (C_7, $–CH_3$), 123.12 (C_α, –CH═CH–), 129.12 ($C_{12,14}$, Ar ring), 129.83 ($C_{11,15}$, Ar ring), 133.26 (C_{10}, Ar ring), 136.49 (C_{13}, C–Cl), 140.66 (C_β, –CH═CH–), 143.26 (C_2, pyrazine ring), 145.66 (C_4, pyrazine ring), 147.45 (C_1, pyrazine ring), 155.17 (C_5, $C–CH_3$) and 190.30 (C_8, –C═O).

(*E*)-3-(4-Bromophenyl)-1-(3-methylpyrazin-2-yl)prop-2-en-1-one (3c)

Molecular formula: $C_{14}H_{11}BrN_2O$; color: yellow crystals; R_f: 0.70; m.p.: 135–137 °C; λ_{max}: 315 and 375 nm; elemental analysis: calculated: C (55.47%), H (3.66%), N (9.24%), O (5.28%); found: C (55.52%), H (3.71%), N (9.23%), O (5.22%); FTIR (KBr, ν_{max} in cm^{-1}): 3038 (Ar, –CH str.); 2969, 2924 (–CH str., $–CH_3$); 1671 (–C═O), 1602 (–C═N), 1561, 1528 (–C═C–), 981 (–C(O)CH═CH), 814 (1,4 substituted Ar ring); +ESIMS: calculated for $C_{14}H_{12}BrN_2O^+$ 303.0054, found 303.0133; ^{1}H NMR (500 MHz, $CDCl_3$, δ ppm): 2.91 (s, 3H, $–CH_3$), 7.57 (s, 4H, $H_{11,12,14,15}$), 7.79–7.76 (d, 1H, J = 16.5 Hz, H_α), 8.02–7.99 (d, 1H, J = 16.0 Hz, H_β), 8.56 (s, 1H, H_2), 8.65 (s, 1H, H_1); ^{13}C NMR (125 MHz, $CDCl_3$, δ ppm): 23.49 (C_7, $–CH_3$), 123.27 (C_α, –CH═CH–), 125.03 (C_{13}, C–Br), 130.08 ($C_{11,15}$, Ar ring), 132.16 ($C_{12,14}$, Ar ring), 133.72 (C_{10}, Ar ring), 140.70 (C_β, –CH═CH–), 143.46 (C_2, pyrazine ring), 145.75 (C_4, pyrazine ring), 147.54 (C_1, pyrazine ring), 155.25 (C_5, $C–CH_3$) and 190.45 (C_8, –C═O).

(*E*)-3-(4-Nitrophenyl)-1-(3-methylpyrazin-2-yl)prop-2-en-1-one (3d)

Molecular formula: $C_{14}H_{11}N_3O_3$; color: yellow crystals; R_f: 0.69; m.p.: 191–193 °C; λ_{max}: 315 and 390 nm; elemental analysis:

calculated: C (62.45%), H (4.12%), N (15.61%), O (17.83%); found: C (62.39%), H (4.17%), N (15.69%), O (17.89%); FTIR (KBr, ν_{max} in cm^{-1}): 3063 (Ar, –CH str.); 2973, 2921 (–CH str., $–CH_3$); 1679 (–C═O), 1614 (–C═N), 1593, 1516 (–C═C), 1516, 1344 (Ar–NO_2), 981 (–C(O)CH═CH), 838 (1,4-substituted Ar ring); +ESIMS: calculated for $C_{14}H_{12}N_3O_3^+$ 270.0800, found 270.0892; ^{1}H NMR (500 MHz, $CDCl_3$, δ ppm): 2.95 (s, 3H, $–CH_3$), 7.89–7.85 (d, 1H, J = 17.0 Hz, H_α), 7.89–7.87 (d, 2H, J = 9.0 Hz, $H_{11,15}$), 8.22–8.19 (d, 1H, J = 16.0 Hz, H_β), 8.32–8.30 (d, 2H, J = 8.5 Hz, $H_{12,14}$), 8.59 (s, 1H, H_2), 8.69 (s, 1H, H_1); ^{13}C NMR (125 MHz, $CDCl_3$, δ ppm): 23.58 (C_7, $–CH_3$), 124.20 (C_α, –CH═CH–), 126.46 ($C_{12,14}$ Ar ring), 129.23 ($C_{11,15}$, Ar ring), 140.82 (C_{10}, Ar ring), 141.03 (C_β, –CH═CH–), 141.44 (C_2, pyrazine ring), 146.13 (C_{13}, C–NO_2), 146.98 (C_4, pyrazine ring), 148.65 (C_1, pyrazine ring), 155.69 (C_5, pyrazine ring) and 190.04 (C_8, –C═O).

(*E*)-3-[4-(Dimethylamino)phenyl]-1-(3-methylpyrazin-2-yl)prop-2-en-1-one (3e)

Molecular formula: $C_{16}H_{17}N_3O$; color: saffron; R_f: 0.83; m.p.: 113–115 °C; λ_{max}: 310 and 510 nm; elemental analysis: calculated: C (71.89%), H (6.41%), N (15.72%), O (5.98%); found: C (71.92%), H (6.38%), N (15.68%), O (6.02%); FTIR (KBr, ν_{max} in cm^{-1}): 3034 (Ar, –CH str.); 2912, 2822 (–CH str., $–CH_3$), 1655 (–C═O), 1618 (–C═N), 1581, 1528 (–C═C), 1373, 1332 (C–N), 989 (–C(O)CH═CH), 842 (1,4-substituted Ar ring); +ESIMS: calculated for $C_{16}H_{18}N_3O^+$ 268.1371, found 268.1470; ^{1}H NMR (500 MHz, $CDCl_3$, δ ppm): 2.86 (s, 3H, $–CH_3$), 3.08 (s, 6H, $–N(CH_3)_2$), 6.72–6.70 (d, 2H, J = 9.0 Hz, $H_{12,14}$), 7.60–7.58 (d, 2H, J = 9.0 Hz, $H_{11,15}$), 7.64–7.61 (d, 1H, J = 16.0 Hz, H_α), 7.79–7.76 (d, 1H, J = 16.0 Hz, H_β), 8.53 (s, 1H, H_2), 8.60 (s, 1H, H_1); ^{13}C NMR (125 MHz, $CDCl_3$, δ ppm): 23.12 (C_7, $–CH_3$), 40.11 ($–N(CH_3)_2$), 111.97–111.75 ($C_{11,14}$ Ar ring), 118.02 (C_α, –CH═CH–), 122.50 (C_{10}, Ar ring), 130.91 ($C_{11,15}$, Ar ring), 140.60 (C_β, –CH═CH–), 144.97 (C_2, pyrazine ring), 146.80 (C_4, pyrazine ring), 149.43 (C_1, pyrazine ring), 152.27 (C_5, pyrazine ring), 154.41 (C_{13}, C–$N(CH_3)_2$) and 191.12 (C_8, –C═O).

(*E*)-3-[4-(Benzyloxy)phenyl]-1-(3-methylpyrazin-2-yl)prop-2-en-1-one (3f)

Molecular formula: $C_{21}H_{18}N_2O_2$; color: yellow crystal; R_f: 0.77; m.p.: 140–142 °C; λ_{max}: 310 and 415 nm; elemental analysis: calculated: C (76.34%), H (5.49%), N (8.48%), O (9.69%); found: C (76.39%), H (5.55%), N (8.54%), O (9.62%); FTIR (KBr, ν_{max} in cm^{-1}): 3034 (Ar, –CH str.); 2922, 2871 (–CH str., $–CH_3$), 1691 (–C═O), 1663 (–C═N), 1585, 1565, 1512 (–C═C–), 1247–1177 (–C–O–C bond linkage of Ar rings) 1002 (–C(O)CH═CH), 838 (1,4 substituted Ar ring), 736-610 (terminal mono-substituted Ar ring); +ESIMS: calculated for $C_{21}H_{19}N_2O_2^+$ 331.1368, found 331.1472; ^{1}H NMR (500 MHz, $CDCl_3$, δ ppm): 2.86 (s, 3H, $–CH_3$), 5.12 (s, 2H, $–OCH_2$), 7.01–6.99 (d, 2H, J = 9.0 Hz, $H_{12,14}$, Ar ring), 7.36–7.33 (d, 1H, J = 13.5 Hz, H_α, –CH═CH–), 7.44–7.39 (m, 4H, $H_{19,20,21}$, Ar ring and H_β, –CH═CH–), 7.64–7.62 (d, 2H, J = 9.0 Hz, $H_{18,22}$, Ar ring), 7.79–7.78 (d, 2H, J = 3 Hz, $H_{11,15}$), 8.52 (s, 1H, pyrazine-H_2), 8.60 (s, 1H, pyrazine-H_1); ^{13}C NMR (125 MHz, $CDCl_3$, δ ppm): 23.33 (C_7, $–CH_3$), 70.13 (C_{16}, $–O–CH_2–$), 115.30 ($C_{12,14}$, Ar ring), 120.87 (C_α, –CH═CH–), 127.51 ($C_{18,22}$, Ar ring), 127.80 (C_{10}, Ar ring), 128.20 (C_{20}, Ar ring), 128.69 ($C_{19,21}$, Ar ring), 130.65 ($C_{11,15}$, Ar ring), 136.38 (C_{17}, Ar ring), 140.67 (C_β, –CH═CH–), 145.13 (C_2, pyrazine), 145.42 (C_4, pyrazine), 148.41 (C_1, pyrazine), 154.88 (C_5, pyrazine), 161.08 (C_{13}, Ar ring) and 190.93 (C_8, –C═O).

(*E*)-1-(3-Ethylpyrazin-2-yl)-3-(4-fluorophenyl)prop-2-en-1-one (3g)

Molecular formula: $C_{15}H_{13}FN_2O$; color: yellow crystal; R_f: 0.70; m.p.: 105–107 °C; λ_{max}: 310 and 365 nm; elemental analysis: calculated: C (70.30%), H (5.11%), N (10.93%), O (6.24%); found: C (70.34%), H (5.20%), N (10.88%), O (6.29%); FTIR (KBr, ν_{max} in cm^{-1}): 3071, 2981 (Ar, –CH str.); 2932, 2879 (–CH str., $–CH_2CH_3$), 1675 (–C═O), 1610 (–C═N), 1585, 1504 (–C═C–), 1014 (–C(O)CH═CH), 830, 802 (1,4-substituted Ar ring); +ESIMS: calculated for $C_{15}H_{13}FN_2O^+$ 257.1012, found 257.1128; ^{1}H NMR (500 MHz, $CDCl_3$, δ ppm): 1.39–1.36 (t, 3H, J = 7.5 Hz, $–CH_3$), 3.24–3.20 (q, 2H, J = 7.5 Hz, $–CH_2$), 7.15–7.12 (t, 2H, J = 8.5 Hz, $H_{12,16}$, Ar ring), 7.70–7.68 (m, 2H, $H_{13,15}$, Ar ring), 7.86–7.76 (dd, 2H, J_{H_β} = 16.0 Hz, J_{H_α} = 16.5 Hz, H_α and H_β, –CH═CH–), 8.55–8.54 (d, 1H, J = 2.5 Hz, pyrazine-H_2), 8.69–8.68 (d, 1H, J = 2.5 Hz, pyrazine-H_1); ^{13}C NMR (125 MHz, $CDCl_3$, δ ppm): 13.35 (C_8, $–CH_3$), 28.79 (C_7, $–CH_2$), 116.22–116.05 ($C_{13,15}$, Ar ring), 123.05–123.03 (C_α, –CH═CH), 130.74–130.67 ($C_{12,16}$, Ar ring), 131.05–131.03 (C_{11}, Ar ring), 140.55 (C_2, pyrazine), 143.94 (C_β, –CH═CH–), 145.74 (C_4, pyrazine), 148.01 (C_1, pyrazine), 159.59 (C_5, pyrazine), 163.21 (C_{14}, Ar ring), and 190.84 (C_9, –C═O).

(*E*)-3-(4-Chlorophenyl)-1-(3-ethylpyrazin-2-yl)prop-2-en-1-one (3h)

Molecular formula: $C_{15}H_{13}ClN_2O$; color: yellow crystals; R_f: 0.78; m.p.: 114–116 °C; λ_{max}: 315 and 375 nm; elemental analysis: calculated: C (66.06%), H (4.80%), N (10.27%), O (5.87%); found: C (66.04%), H (4.77%), N (10.20%), O (5.94%); FTIR (KBr, ν_{max} in cm^{-1}): 3081, 2980 (Ar C–H str.); 2928, 2880 (–CH str., $–CH_2CH_3$), 1672 (–C═O), 1605 (–C═N), 1564, 1486 (–C═C–), 1009 (–C(O)CH═CH), 830, 804 (1,4-substituted Ar ring); +ESIMS: calculated for $C_{15}H_{13}ClN_2O^+$ 273.0716, found 273.0831; ^{1}H NMR (500 MHz, $CDCl_3$, δ ppm): 1.39–1.36 (t, 3H, J = 7.5 Hz, $–CH_3$), 3.24–3.20 (q, 2H, J = 7.5 Hz, $–CH_2$), 7.42–7.41 (d, 2H, J = 8.5 Hz, $H_{12,16}$, Ar ring), 7.64–7.62 (d, 2H, J = 8.5 Hz, $H_{13,15}$, Ar ring), 7.78–7.75 (d, 1H, J = 16.0 Hz, H_α, –CH═CH–), 7.92–7.88 (d, 1H, J = 16.0 Hz, H_β, –CH═CH–), 8.55–8.55 (d, 1H, J = 2.0 Hz, pyrazine-H_2), 8.69–8.69 (d, 1H, J = 2.0 Hz, pyrazine-H_1); ^{13}C NMR (125 MHz, $CDCl_3$, δ ppm): 13.33 (C_8, $–CH_3$), 28.81 (C_7, $–CH_2$), 123.70 (C_α, –CH═CH), 129.24 ($C_{12,16}$, Ar ring), 129.90 ($C_{13,15}$, Ar ring), 133.28 (C_{11}, Ar ring), 136.68 (C_{14}, Ar ring), 140.56 (C_2, pyrazine), 143.66 (C_β, –CH═CH–), 145.81 (C_4, pyrazine), 147.84 (C_1, pyrazine), 159.69 (C_5, pyrazine), and 190.74 (C_9, –C═O).

(*E*)-3-(4-Bromophenyl)-1-(3-ethylpyrazin-2-yl)prop-2-en-1-one (3i)

Molecular formula: $C_{15}H_{13}BrN_2O$; color: yellow crystals; R_f: 0.81; m.p.: 95–97 °C; λ_{max}: 305 and 375 nm; elemental analysis:

calculated: C (56.80%), H (4.13%), N (8.83%), O (5.04%); found: C (56.84%), H (4.19%), N (8.78%), O (5.09%); FTIR (KBr, ν_{max} in cm^{-1}): 3077, 2977 (Ar, –CH str.); 2932, 2872 (–CH str., $–CH_2CH_3$), 1672 (–C═O), 1601 (–C═N), 1583, 1531 (–C═C–), 1005 (–C(O)CH═CH), 856, 800 (1,4-substituted Ar ring); +ESIMS: calculated for $C_{15}H_{13}BrN_2O^+$ 317.0211, found 317.0324; ^{1}H NMR (500 MHz, $CDCl_3$, δ ppm): 1.39–1.36 (t, 3H, J = 7.5 Hz, $–CH_3$), 3.24–3.20 (q, 2H, J = 7.5 Hz, $–CH_2$), 7.59–7.54 (q, 4H, J = 8.5 Hz, $H_{12,13,15,16}$, Ar ring), 7.76–7.73 (d, 1H, J = 16.5 Hz, H_α, –CH═CH–), 7.93–7.90 (d, 1H, J = 16.0 Hz, H_β, –CH═CH–), 8.55–8.55 (d, 1H, J = 2.5 Hz, pyrazine-H_2), 8.69–8.69 (d, 1H, J = 2.5 Hz, pyrazine-H_1); ^{13}C NMR (125 MHz, $CDCl_3$, δ ppm): 13.33 (C_8, $–CH_3$), 28.81 (C_7, $–CH_2$), 123.79 (C_α, –CH═CH), 125.09 (C_{14}, Ar ring), 130.09 ($C_{12,16}$, Ar ring), 132.20 ($C_{13,15}$, Ar ring), 133.70 (C_{11}, Ar ring), 140.56 (C_2, pyrazine), 143.71 (C_β, –CH═CH–), 145.83 (C_4, pyrazine), 147.81 (C_1, pyrazine), 159.70 (C_5, pyrazine), and 190.73 (C_9, –C═O).

(*E*)-1-(3-Ethylpyrazin-2-yl)-3-(4-nitrophenyl)prop-2-en-1-one (3j)

Molecular formula: $C_{15}H_{13}N_3O_3$; color: yellow crystals; R_f: 0.68; m.p.: 199–201 °C; λ_{max}: 295 and 380 nm; elemental analysis: calculated: C (63.60%), H (4.63%), N (14.83%), O (16.94%); found: C (63.66%), H (4.70%), N (14.77%), O (16.95%); FTIR (KBr, ν_{max} in cm^{-1}): 3103, 2980 (Ar, –CH str.); 2936, 2880 (–CH str., $–CH_2CH_3$), 1676 (–C═O), 1613 (–C═N), 1594, 1516.10 (–C═C–), 1344, 1315 ($–C–NO_2$), 1005 (–C(O)CH═CH), 860, 845 (1,4-substituted Ar ring); +ESIMS: calculated for $C_{15}H_{13}N_3O_3^+$ 284.0957, found 284.1069; ^{1}H NMR (500 MHz, $CDCl_3$, δ ppm): 1.40–1.37 (t, 3H, J = 7.5 Hz, $–CH_3$), 3.29–3.24 (q, 2H, J = 7.5 Hz, $–CH_2$), 7.86–7.83 (br, 3H, $J_{H_{12},H_{16}}$ = 9.0 Hz, J_{H_α} = 16.0 Hz, $H_{12,16}$, Ar ring and H_α, –CH═CH–), 8.15–8.12 (d, 1H, J = 16.0 Hz, H_β, –CH═CH–), 8.31–8.29 (d, 2H, J = 9.0 Hz, $H_{13,15}$ Ar ring), 8.58–8.57 (d, 1H, J = 2.0 Hz, pyrazine-H_2), 8.72–8.72 (d, 1H, J = 2.5 Hz, pyrazine-H_1); ^{13}C NMR (125 MHz, $CDCl_3$, δ ppm): 13.25 (C_8, $–CH_3$), 28.92 (C_7, $–CH_2$), 124.20 (C_α, –CH═CH), 126.84 ($C_{13,15}$, Ar ring), 129.22 ($C_{12,16}$, Ar ring), 140.63 (C_{11}, Ar ring), 140.99 (C_2, pyrazine), 141.50 (C_β, –CH═CH–), 146.22 (C_4, pyrazine), 147.03 (C_{14}, Ar ring), 148.64 (C_1, pyrazine), 160.18 (C_5, pyrazine), and 190.12 (C_9, –C═O).

(*E*)-3-(4-(Dimethylamino)phenyl)-1-(3-ethylpyrazin-2-yl)prop-2-en-1-one (3k)

Molecular formula: $C_{17}H_{19}N_3O$; color: light saffron; R_f: 0.82; m.p.: 105–107 °C; λ_{max}: 295 and 510 nm; elemental analysis: calculated: C (72.57%), H (6.81%), N (14.94%), O (5.69%); found: C (72.60%), H (6.77%), N (14.98%), O (5.72%); FTIR (KBr, ν_{max} in cm^{-1}): 3081, 2980 (Ar, –CH); 2924, 2816 (–CH str., $–CH_2CH_3$), 1657 (–C═O), 1613 (–C═N), 1564, 1523 (–C═C), 1363, 1333 (–C–N), 1009 (–C(O)CH═CH), 856, 826 (1,4-substituted Ar ring); +ESIMS: calculated for $C_{17}H_{19}N_3O^+$ 282.1528, found 282.1667; ^{1}H NMR (500 MHz, $CDCl_3$, δ ppm): 1.38–1.35 (t, 3H, J = 7.5, $–CH_3$), 3.08 (s, 6H, $–N(CH_3)_2$), 3.18–3.13 (q, 2H, J = 7.5, $–CH_2$), 6.71–6.69 (d, 2H, J = 8.5 Hz, $H_{13,15}$, Ar ring), 7.53–7.50 (d, 1H, J = 16.0 Hz, H_α, –CH═CH–), 7.58–7.56 (d, 2H, J = 9.0 Hz, $H_{12,16}$, Ar ring), 7.73–7.70 (d, 1H, J = 15.5 Hz, H_β, –CH═CH–), 8.52–8.52 (d, 1H, J = 2.0 Hz, pyrazine-H_2), 8.64–8.63 (d, 1H, J = 2.0 Hz, pyrazine-H_1); ^{13}C NMR (125 MHz, $CDCl_3$, δ ppm): 13.47 (C_8, $–CH_3$), 28.59 (C_7, $–CH_2$), 40.10 $N(CH_3)_2$, 111.74 ($C_{13,15}$, Ar ring), 118.51 (C_α, –CH═CH), 122.37 (C_{11}, Ar ring), 130.91 ($C_{12,16}$, Ar ring), 140.50 (C_2, pyrazine), 145.02 (C_β, –CH═CH–), 147.06 (C_4, pyrazine), 149.71 (C_1, pyrazine), 152.28 (C_{14}, Ar ring), 158.75 (C_5, pyrazine), and 191.42 (C_9, –C═O).

(*E*)-3-(4-(Benzyloxy)phenyl)-1-(3-ethylpyrazin-2-yl)prop-2-en-1-one (3l)

Molecular formula: $C_{22}H_{20}N_2O_2$; color: yellow crystals; R_f: 0.81; m.p.: 118–120 °C; λ_{max}: 250 and 420 nm; elemental analysis: calculated: C (76.72%), H (5.85%), N (8.13%), O (9.29%); found: C (76.66%), H (5.90%), N (8.18%), O (9.26%); FTIR (KBr, ν_{max} in cm^{-1}): 3088, 2977 (Ar, –CH); 2936, 2872 (–CH str., $–CH_2CH_3$), 1665 (–C═O), 1590 (–C═N), 1568, 1508 (–C═C–), 1292, 1180 (–C–O–C bond linkage of Ar rings), 1013 (–C(O)CH═CH), 878, 800 (1,4-substituted Ar ring), 729, 610 (terminal mono-substituted Ar ring); +ESIMS: calculated for $C_{22}H_{20}N_2O_2^+$ 345.1525, found 345.1648; ^{1}H NMR (500 MHz, $CDCl_3$, δ ppm): 1.39–1.36 (t, 3H, J = 7.5 Hz, $–CH_3$), 3.22–3.17 (q, 2H, J = 7.5 Hz, $–CH_2$), 5.14 (s, 2H, $–OCH_2$), 7.04–7.02 (d, 2H, J = 9.0 Hz, $H_{13,15}$, Ar ring), 7.39–7.36 (t, 1H, J = 7.0 Hz, H_{21}, terminal Ar ring), 7.47–7.41 (m, 4H, $H_{19,20,22,23}$ terminal Ar ring), 7.65–7.64 (d, 2H, J = 8.5 Hz, $H_{12,16}$ Ar ring), 7.78–7.70 (br, 2H, J_{H_α} = 16.0 Hz, J_{H_β} = 16.0 Hz, H_β and H_α –CH═CH–), 8.54–8.53 (d, 1H, J = 2.0 Hz, pyrazine-H_2), 8.67–8.66 (d, 1H, J = 2.0 Hz, pyrazine-H_1); ^{13}C NMR (125 MHz, $CDCl_3$, δ ppm): 13.42 (C_8, $–CH_3$), 28.73 (C_7, $–CH_2$), 70.13 (C_{17}, $–OCH_2$), 115.30 ($C_{13,15}$, Ar ring), 121.34 (C_α, –CH═CH), 127.51 ($C_{19,23}$, terminal Ar ring), 127.72 (C_{21}, terminal Ar ring), 128.22 ($C_{12,16}$, Ar ring), 128.70 (C_{11}, Ar ring), 130.66 ($C_{20,22}$, terminal Ar ring), 136.36 (C_{18}, Ar ring), 140.54 (C_2, pyrazine), 145.38 (C_β, –CH═CH–), 145.47 (C_4, pyrazine), 148.66 (C_1, pyrazine), 159.27 (C_5, pyrazine), 161.10 (C_{14}, Ar ring), and 191.20 (C_9, –C═O).

Notes and references

1 F. Wenlai, X. Yan and Z. Yanhong, *J. Agric. Food Chem.*, 2007, **55**, 9956.
2 T. S. David and C. Peter, *Anal. Chem.*, 1989, **61**, 1328.
3 Z. Michael, *Aroma Chemicals II: Heterocycles*, in *Chemistry and technology of flavors and fragrances*, ed. D. J. Rowe, Blackwell Publishing Ltd., UK, 1st edn, 2005, p. 108.
4 P. Gosh and P. Mandal, *Green Chem. Lett. Rev.*, 2012, **5**, 127.
5 X. A. Wu, Y. M. Zhao and N. J. Yu, *J. Asian Nat. Prod. Res.*, 2007, **9**, 437.
6 K. Zurbonsen, A. Michel, P. A. Bonnet, M. N. Mathieu and C. Chevillard, *Gen. Pharmacol.*, 1999, **32**, 135.
7 Z. Zhaohui, W. Taotao, H. Jingwu, L. Gengshan, Y. Shaozu and X. Wenjuan, *Life Sci.*, 2003, **72**, 2465.
8 F. Pilar, E. Cristina, T. Lorena, A. A. Juan, O. Adelina, M. Monica, C. Cristina, R. Isabel, L. Manel, M. Montserrat and V. Bernat, *Bioorg. Med. Chem. Lett.*, 2012, **22**, 2784.
9 G. K. Yoon, K. C. Min, W. K. Jong, H. K. Dong, G. K. Sang and G. L. Myung, *Int. J. Pharm.*, 2003, **255**, 1.

10 C. S. Mizuno, S. Paul, N. Suh and A. M. Rimando, *Bioorg. Med. Chem. Lett.*, 2010, **20**, 7385.
11 B. P. Bandgar, S. S. Gawande, R. G. Bodade, N. M. Gawande and C. N. Khobragade, *Bioorg. Med. Chem.*, 2009, **17**, 8168.
12 S. H. Lee, D. H. Sohn, X. Y. Jin, S. W. Kim, S. C. Choi and G. S. Seo, *Biochem. Pharmacol.*, 2007, **74**, 870.
13 M. V. B. Reddy, W. Tsai, K. Qian, K. H. Lee and T. S. Wu, *Bioorg. Med. Chem.*, 2011, **19**, 7711.
14 A. Bhattacharya, L. C. Mishra, M. Sharma, S. K. Awasthi and V. K. Bhasin, *Eur. J. Med. Chem.*, 2009, **44**, 3388.
15 H. Shi, S. Zhang, Q. Ge, D. Guo, C. Cai and W. Hua, *Bioorg. Med. Chem. Lett.*, 2010, **20**, 6555.
16 B. Insuasty, A. Tigreros, F. Orozco, J. Quiroga, R. Abonia, M. Nogueras, A. Sanchez and J. Cobo, *Bioorg. Med. Chem.*, 2010, **18**, 4965.
17 M. Liu, P. Wilairat, S. L. Croft, A. L. Tan and M. Go, *Bioorg. Med. Chem.*, 2003, **11**, 2729.
18 K. Liaras, A. Geronikaki, J. Glamoclija, A. Ciric and M. Sokovic, *Bioorg. Med. Chem.*, 2011, **19**, 3135.
19 A. M. Deshpande, N. P. Argadea, A. A. Natua and J. Eckman, *Bioorg. Med. Chem.*, 1999, **7**, 1237.
20 S. Horrick, P. Shivaputra, W. S. Tino, N. Nouri, F. S. Raymond and K. B. John, *Bioorg. Med. Chem.*, 2011, **19**, 2030.
21 K. M. Vijay, C. Vinita, S. Shubhra, S. Shyam, S. Sudhir and B. Kalpana, *Eur. J. Med. Chem.*, 2011, **46**, 4302.
22 R. Kumar, P. Sharma, A. Shard, D. K. Tewary, G. Nadda and A. K. Sinha, *Med. Chem. Res.*, 2012, **21**, 922.
23 M. Kidwai and P. Misra, *Synth. Commun.*, 1999, **29**, 3237.
24 D. Azarifar and H. Ghasemnejad, *Molecules*, 2003, **8**, 642.
25 Z. N. Siddiqui, T. N. M. Musthafa, A. Ahmad and A. U. Khan, *Bioorg. Med. Chem. Lett.*, 2011, **21**, 2860.
26 S. Sebti, A. Solhy, A. Smahi, A. Kossir and H. Oumimoum, *Catal. Commun.*, 2002, **3**, 335.
27 Q. Xu, Z. Yang, D. Yin and F. Zhang, *Catal. Commun.*, 2008, **9**, 1579.
28 O. Petrov, Y. Ivanova and M. Gerova, *Catal. Commun.*, 2008, **9**, 315.
29 N. B. Pathan, A. M. Rahatgaonkar and M. S. Chorghade, *Catal. Commun.*, 2011, **12**, 1170.
30 P. E. More, B. P. Bandgar and V. T. Kamble, *Catal. Commun.*, 2012, **27**, 30.
31 L. B. Kunde, S. M. Gade, V. S. Kalyani and S. P. Gupte, *Catal. Commun.*, 2009, **10**, 1881.
32 C. M. Comisar and P. E. Savage, *Green Chem.*, 2004, **6**, 227.
33 M. Ozil and M. Canpolat, *Polyhedron*, 2013, **51**, 82.
34 R. S. Varma, *Green Chem.*, 1999, **1**, 43.
35 N. Singh, S. K. Singh, R. S. Khanna and K. N. Singh, *Tetrahedron Lett.*, 2011, **52**, 2419.
36 P. F. Wang, N. O. Komatsuzaki, Y. Himeda, H. Sugihara, H. Arakawa and K. Kasuga, *Tetrahedron Lett.*, 2001, **42**, 9199.
37 Z. J. Ning, Q. Zhang, H. C. Pei, J. F. Luan, C. G. Lu and Y. P. Cui, *J. Phys. Chem. C*, 2009, **113**, 10307.
38 Y. F. Sun and Y. P. Cui, *Dyes Pigm.*, 2009, **81**, 27.
39 P. Skehn, R. Storeng, A. Scudiero, J. Monks, D. McMohan, D. Vistica, T. W. Jonathan, H. Bokesch, S. Kenney and M. R. Boyd, *J. Natl. Cancer Inst.*, 1990, **82**, 1107.
40 M. C. Suzanne, G. P. Peter, A. S. Richard and R. P. Don, *J. Biol. Chem.*, 1996, **271**, 5422.
41 S. George, M. Parameswaran, A. R. Chakraborty and T. K. Ravi, *Acta Pharm.*, 2008, **58**, 119.
42 L. A. Chitwood, *Appl. Microbiol.*, 1969, **17**, 707.
43 E. Balnois and K. J. Wilkinson, *Colloids Surf., A*, 2002, **207**, 229.
44 A. Dubes, H. P. Lopez, W. Abdelwahed, G. Degobert, H. Fessi, P. Shahgaldian and A. W. Coleman, *Eur. J. Pharm. Biopharm.*, 2003, **55**, 279.
45 M. Skerget, Z. Knez and M. Knez-Hrncic, *J. Chem. Eng. Data*, 2011, **56**, 694.
46 (*a*) M. Singh, *J. Biochem. Biophys. Methods*, 2006, **67**, 151; (*b*) M. Singh, *Surf. Rev. Lett.*, 2007, **14**, 973; (*c*) M. Singh and Sushma, *J. Mol. Liq.*, 2009, **148**, 6.
47 OSIRIS, Drug-Relevant Properties Prediction, July 2012, http://www.rdchemicals.com/drug-relevant-properties.html.

